# Environmental Science
## Processes & Impacts

Accepted Manuscript






ROYAL SOCIETY OF CHEMISTRY

rsc.li/process-impacts

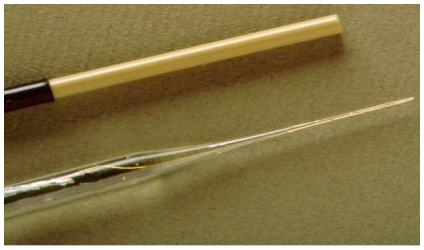

*In situ* voltammetry used for chemical analysis of a variety of habitats for Iron(II) oxidizing bacteria; freshwater to hydrothermal vents.

Environmental Impact Statement

Here, *in situ* voltammetry is used as a tool to help better understand the role iron oxidizing bacteria (FeOB) have in the biogeochemistry of iron in a variety of aqueous environments, both fresh and saline. By measuring redox species such as Fe(II), Fe(III), and $O_2$ *in situ,* it was possible to locate areas where FeOB would occupy. The simultaneous measurements of the previously mentioned redox species also allowed for the characterization of environments where typical orange – red iron oxyhydroxide microbial mats were visible. Studies such as this are important as there is still much to be understood with biotically mediated Fe(II) oxidation and other processes they are involved in.

Environmental Science: Processes & Impacts RSCPublishing

ARTICLE

# Using *in situ* voltammetry as a tool to identify and characterize habitats of iron-oxidizing bacteria: from fresh water wetlands to hydrothermal vent sites

Cite this: DOI: 10.1039/x0xx00000x

Received 00th January 2012,
Accepted 00th January 2012

DOI: 10.1039/x0xx00000x

www.rsc.org/

*Daniel J. MacDonald[1], Alyssa J. Findlay[2], Sean M. McAllister[2], Josh M. Barnett[3], Patricia Hredzak-Showalter[2], Sean T Krepski[3], Shane G. Cone[3], Jarrod Scott[4], Sarah K. Bennett[2], Clara S. Chan[2,3], David Emerson[4], George W. Luther III[1,2]*

1. *Department of Chemistry and Biochemistry, University of Delaware, Newark, Delaware USA.*
2. *School of Marine Science and Policy, University of Delaware, Lewes, Delaware USA.*
3. *Department of Geological Sciences, University of Delaware, Newark, Delaware USA.*
4. *Bigelow Laboratory for Ocean Sciences, East Boothbay, ME, USA*

## *Abstract*

Iron-oxidizing bacteria (FeOB) likely play a large role in the biogeochemistry of iron, making the detection and understanding of the biogeochemical processes FeOB are involved in of critical importance. By deploying our in situ voltammetry system, we are able to measure a variety of redox species, specifically $Fe^{2+}$ and $O_2$, simultaneously. This technique provides significant advantages in both characterizing the environments in which microaerophilic FeOB are found, and finding diverse conditions in which FeOB could potentially thrive. Described here are four environments with different salinities [one fresh groundwater seep site, one beach-groundwater mixing site, one hydrothermal vent site (Mid-Atlantic Ridge), and one estuary (Chesapeake Bay)] where *in situ* voltammetry was deployed, and where the presence of FeOB were confirmed by either culturing methods or molecular data. The sites varied in both $O_2$ and Fe(II) content with $O_2$ ranging from below the 3 μM detection limit of the electrodes at the Chesapeake Bay suboxic zone, to as high 150 μM $O_2$ at the vent site. In addition, a range of Fe(II) concentrations supported FeOB communities, from 3μM Fe(II) in the Chesapeake Bay to 300μM in the beach aquifer. *In situ* electrochemistry provides the means to quickly measure these redox gradients at appropriate resolution, making it possible in real time to detect niches likely inhabited by microaerophilic FeOB, then accurately sample for proof of FeOB presence and activity. This study demonstrates the utility of this approach while also greatly expanding our knowledge of FeOB habitats.

## Introduction

### 1.0 Introduction

In this paper we describe several different natural environment sites with varying salinity content ranging from freshwater to fully saline ocean water where, using *in situ* methods we sought to find neutrophilic, microaerophilic iron (II)-oxidizing bacteria (FeOB) and characterize the environments in which they are found for further research and study. FeOB are implicated in important redox processes both on modern Earth, specifically Fe(III) oxyhydroxide precipitation and associated contaminant and nutrient sequestration[1,2], and ancient Earth, including possible contribution to the extensive banded iron formations[3,4], whose formation mechanism is greatly debated. While FeOB appear to prefer certain Fe(II) and $O_2$ concentration ranges, this knowledge comes from relatively few culture studies and environmental studies that are mostly restricted to freshwater sites and a few marine hydrothermal sites[5,6]. Here we show how *in situ* voltammetry can help us broaden the range of known FeOB habitats and constrain the Fe(II) and $O_2$ concentrations associated with FeOB.

Understanding the $O_2$ range of FeOB is particularly important for understanding the biogeochemical history of the Earth. The appearance and rise in atmospheric oxygen ~2.3 billion years ago led to dramatic changes in the oceanic iron cycle; it has been proposed that rapid reaction of Fe(II) with $O_2$ would form Fe(III), such that Fe(II) would be removed from oxic waters. However, before the appearance of $O_2$, Fe(II) oxidation could have been mediated under anoxic conditions by bacterial anoxygenic photosynthesis [photoferrotrophy][1,7] or, under very low oxygen conditions, mediated by microaerophilic FeOB using $O_2$ produced by cyanobacteria and before $O_2$ built up to high concentrations. At zero to low oxygen concentrations, these two microbial processes would have been faster than chemical oxidation[8,9] , and could still have resulted in Fe mineralization, accumulating geologic-scale iron formations. We have previously shown that voltammetry can be used to discriminate between various abiotic and biotic Fe oxidation processes, as described below. This paper focuses on aerobic FeOB in a range of modern environments where oxygen concentrations are variable but low, potentially similar to ancient environments.

To better understand the niches that FeOB currently occupy, *in situ* voltammetry was utilized in several environments where Fe(II) and oxygen concentrations were expected to overlap. *In situ* analyzers are ideal for this type of study because data on multiple chemical species can be collected quickly, enabling more accurate, discrete sampling of organisms and other chemical species when compared to traditional techniques (e.g. spectroscopy). Our voltammetry system, which can detect $O_2$ and Fe(II) simultaneously, was deployed at four different sites where we suspected the presence of active FeOB. The study sites included one freshwater site (Lakeside Drive Boothbay Harbor, ME), one marine site (Mid Atlantic Ridge vent sites), one intertidal groundwater mixing environment (Cape Shores Beach, Lewes, DE), and an estuary (Chesapeake Bay).

Microaerophilic iron-oxidizing bacteria were present at all sites across different salinities and varying oxygen and iron levels. FeOB in fresh surface water habitats are better characterized, probably because they are easily accessible[10–13]. Less is known about FeOB in estuarine, coastal, and oceanic environments, and preliminary findings confirming their presence are reported here; however, the primary focus of this paper is on characterization of chemical gradients and conditions within these environments. Important differences in these sites include simple vertical stratification that occurs in the Chesapeake Bay and at microbial mats near hydrothermal vents, versus horizontal movement of water containing iron that occurs along creek side banks and seeps, as well as more complex flow paths within the intertidal zone mixing of fresh groundwater penetrating through beach sands and interacting with ocean waters. In these environments, iron, oxygen, and other chemical gradients are a combined result of physical hydrology, chemical, and biological processes; *in situ* voltammetry can help us understand the interaction of these processes, and the response of FeOB to these gradients.

Work to date shows that freshwater FeOB are typically in the taxonomic class of *Betaproteobacteria*, whereas marine FeOB are members of the class *Zetaproteobacteria*[14]. In both fresh and marine environments, we confirmed the presence of FeOB by some combination of culturing methods and molecular biological data. Only the freshwater site and the hydrothermal vent sites showed visible proof of orange – red iron(III) oxyhydroxide floc morphology and microscopic structures typical of microbial mats, which are formed as a byproduct of microbial Fe(II) oxidation[15,16]. The precipitated solids form at circumneutral pH as the waste products of iron oxidation by FeOB. However, in several cases, it was not clear whether the oxides were biogenic, necessitating the use of culture and molecular approaches for confirmation FeOB presence.

### 1.1 Biogeochemistry of Iron

Iron is an essential nutrient for all known life forms and a potential energy source for bacteria and archaea. In natural aqueous environments, iron typically exists in two oxidation states [Fe(II) and Fe(III)] where Fe(II) is soluble and Fe(III) is normally a solid in the absence of strong ligands or chelates. The form of iron that dominates typically depends on redox conditions and pH[17]. Fe(II) is more abundant in anoxic environments, whereas in oxygenated environments, Fe(III) is more common, as Fe(II) is readily oxidized. After Fe(II) is oxidized, Fe(III) quickly hydrolyzes and, in the absence of organic ligands, precipitates at circumneutral pH. Abiotic oxidation of Fe(II) in oxygenated waters has a half-life of less than 1 minute at 100% oxygen saturation at circumneutral pH (pH~7) (Equation 1)[14], meaning that rapid abiotic oxidation decreases the concentration of soluble Fe(II).

$$(1)\quad -d[Fe^{2+}]/dt = k[Fe^{2+}]\,[O^2]\,[OH^-]^2$$

Under microaerobic (<50 μM) conditions chemical oxidation of Fe(II) slows considerably, allowing the potential for FeOB to utilize Fe(II) as an energy source[14]. This highlights the importance that the surrounding environment can have on iron availability and reactivity. As indicated in Equation 1, another important parameter in iron chemistry is pH. As pH changes, so does the reactivity of iron, with chemical oxidation occurring more rapidly as pH increases. In acidic environments, abiotic oxidation proceeds slowly. The majority of isolated, characterized microorganisms capable of growing on Fe(II) are acidophilic. Because these acidophiles are more well known, FeOB are often considered to grow at pH<4, where Fe(II) is stable in the presence of air saturated solutions; however, they may also occupy environments at circumneutral pH. In microaerobic environments, FeOB experience lower concentrations of oxygen, but constant fluxes of both $O_2$ and Fe(II). As FeOB mediate the transformation of soluble Fe(II) to solid Fe(III), the efficiency at which these organisms are able to do this is dictated by the iron and oxygen concentrations and the gradients (and therefore flux) of each in the environment in which they are found.

Using voltammetry we have previously shown the ability to differentiate between four known Fe(II) oxidation processes in real time. Oxygen concentrations are one key to distinguishing the four mechanisms: the first three require $O_2$ to be present at varying concentrations, while the fourth process requires anoxic conditions.

1) Abiotic, chemical oxidation (equation 1), where $O_2$ is distally-sourced and concentrations are high (e.g. diffuses into environment from atmosphere);

2) Abiotic, but mediated locally by cyanobacteria and not FeOB, which produce high concentrations of $O_2$, but only when light is present (e.g. Chocolate Pot Hot springs in Yellowstone; Trouwborst et. al, 2007[18]);

3) Biotic oxidation mediated by microaerophilic (low $O_2$-requiring) FeOB (e.g. Fe microbial mats at Fe seeps; Druschel et. al, 2008[9]);

4) Anaerobic phototrophs (photoferrotrophs) that oxidize Fe(II) when light is present, but do not use or produce $O_2$. Although the kinetics of process 4 still needs to be characterized, this process does not require $O_2$ to oxidize Fe(II) and thus can be easily distinguished from the other three processes.

Processes 1 and 3 follow pseudo first order kinetics and do not require light for reaction to occur whereas the cyanobacteria-associated process 2 follows zero order kinetics and requires light[19]. Process 4, photoferrotrophy, is expected to follow zero order kinetics as it is a light dependent (mediated) reaction like process 2. Although it has been assumed that abiotic chemical oxidation (process 1) is very common in modern environments, we suggest that Fe(II) and O2 conditions in many environments actually favor microaerophilic Fe oxidation (process 3), which is a motivation for the current study, looking for these microaerophilic FeOB (which we simply refer to as FeOB from hereon) and characterizing their chemical environment.

Based on the results of these previous studies in natural environments, we used *in situ* voltammetry to search for FeOB at three saline sites where there would be low or no light (thus negligible or no cyanobacterial and photoferrotroph activity): (1) MAR at > 2200 meters in the absence of light, (2) Chesapeake Bay low light suboxic zone and (3) an intertidal groundwater mixing environment at Cape Shores, DE in the absence of light. Lastly we chose a freshwater site with low light where there was no significant cyanobacterial activity to raise oxygen concentrations as we found in Trouwborst et al (2007).

## 2.0 Experimental

### 2.1 Voltammetry

We used Au-amalgam microelectrodes that are non-selective and can measure the concentrations *in situ* of a suite of important redox species simultaneously. Our *in situ* electrodes allowed for simultaneous measurement of several key redox species ($O_2$, $H_2O_2$, $Fe^{2+}$, $Fe^{3+}$, $H_2S$, FeS, and $Mn^{2+}$)[20]. Cyclic voltammograms (CV) for these redox species were collected by conditioning the electrode at an initial potential of -0.05 V for 2 s, then scanning from -0.05 to -1.8 V and back to -0.05 V at a scan rate of 2 Volts per second. A conditioning potential of -0.9 V was applied for 5 s before each CV scan to clean the electrode surface and ensure electrode reproducibility and integrity. The 100% $O_2$ current values are determined for each electrode prior to use by using an aquarium bubbler to aerate filtered seawater or freshwater solutions. After the 100% saturation value is determined for the electrode in use, Equation 2 was used to determine the oxygen concentrations at each depth. Oxygen saturation was calculated by using a standard dissolved oxygen equation for each depth with varying temperature and salinity [21].

*(2) 100% $O_2$ saturation (μM) x [($O_2$ current (nA)/100% $O_2$ current (nA)] = [$O_2$] (μM)*

Fe(II) standard curves in the appropriate solution are completed for each electrode used *in situ* prior to use. Fe(III) species can be detected but cannot be quantified as noted in Taillefert et al. (2000)[22]. The detection limits for $O_2$ and Fe(II) are 3 μM and 7 μM, respectively.

### 2.2 Electrode Construction

Two types of electrodes were used as described in Luther et al (2008)[20] and Brendel and Luther (1995)[23]. One design is for the sampling of mats and sediments whereas the other is primarily for water column work. All electrodes are used in conjunction with electrochemical analyzers from Analytical Instrument Systems, Inc.

Gold amalgam glass electrodes are constructed as described in Brendel and Luther (1995) with modifications to insure a waterproof seal. Briefly, the end of a

15 cm section of 5 or 6 mm-diameter glass tubing is heated in a small flame and the tip pulled to a diameter of less than 0.4 mm for a length of about 3–5 cm. The

100 μm-diameter Au wire is soldered to the conductor wire of a BNC cable (RG-174U/type 50 Ω coax cable; 0.095 in diameter) and inserted through the larger inside diameter part of the glass so that the Au/Cu/solder junction is at the bottom of the large diameter part of the glass. Then, the solder junction is fixed within the tubing with West System 105 epoxy resin and 206 hardener to form a high-purity, optical-grade, nonconductive fill. The epoxy is injected into the larger diameter of the glass tubing with a syringe and Teflon cannula (20 gauge). The epoxy drains slowly through the open smaller diameter of the glass tip. On setting, the epoxy seals the tip and the top end can be refilled with epoxy if necessary. After final setting of the epoxy, the tip is sanded and polished. Then the top end is coated with Scotchkote (3M) electrical coating and Scotchfil (3M) electrical insulation putty. These glass tipped electrodes are durable, but can break when dropped or when they hit clam shells, rocks or other hard surfaces in sediments. The wire is then mated to an appropriate connector for attachment to the analyzer.

Durable polyethyletherketone (PEEK) working electrodes are constructed in a similar fashion as above by soldering the 100 μm Au wire directly to a BNC cable and then placing into a 10 cm section of 0.125 inch diameter PEEK tubing. The solder is then fixed in the tubing by adding West System 105 epoxy and 206 hardener.

All working electrodes are then sanded and polished with 4 diamond polishes (15; 6; 1; and 0.25 μm). Once the gold surface has been polished the working electrodes are plated with Hg for 4 minutes at a potential of -0.1V in a solution of 0.1M Hg/.05M $HNO_3$[20].

A 3-electrode system is utilized with the 100 μm Au working electrode prepared in PEEK tubing, a Ag/AgCl as the reference electrode, and a Pt as the counter electrode; the reference and counter are prepared in PEEK as well.

### 2.3 Chesapeake Bay Sensor Package and sampling (July/August 2011 and 2013)

An instrument profiling system capable of measuring high resolution *in situ* vertical profiles of a variety of chemical species and physical parameters was designed and built for deployment from the R\V *Hugh R Sharp* in the Chesapeake Bay. To measure *in situ* chemical species, a DLK sub II In Situ Electrochemical Analyzer (ISEA) designed by Analytical Instrument Systems was used in conjunction with 100 $\mu M$ Au/Hg amalgam PEEK microelectrodes that were prepared as described above. Detection limits for oxygen, sulfide and Fe(II) are 3 μM, 0.2 μM and 7μM respectively. The ISEA controlled a SeaBird SBE 37-SI MicroCAT CTD, which measured salinity, temperature and depth. In addition, a Satlantic *in situ* FIRe (Fluorescence Induction and Relaxation) sensor was used to monitor chlorophyll-a and quantum efficiency of photochemistry in photosystem II, i.e. the health of phytoplankton [24]. Lastly, a photosynthetically active radiation sensor (PAR) was mounted on top of the instrument cage to observe changes in light intensity with depth. The instrument package also contained a marine pump, which was able to pump water from depths up to 20 meters on to the deck of the ship where it could pass through a flow cell for additional analysis. The pump sampling provides 10 cm vertical resolution in the absence of wave action, as opposed to sampling from CTD rosette bottles with a 1 meter depth resolution. The pump profiler consisted of 100 ft of 1/4 in. diameter Teflon tubing attached to a west marine water pump (flow rate of 4160 liters/hour) that was secured on the instrument cage. To improve data correlation, the pump inlet was located at the same depth as the Au/Hg working electrodes and CTD sensor.

### 2.4 Lakeside Drive Sampling (July 17-19, 2012)

Lakeside Drive (Boothbay Harbor, Maine) is bordered to the east by the West Harbor Pond, a salt-water outlet to the Atlantic Ocean, and just meters to the west by a shallow, freshwater creek called Lakeside Drive Creek[25]. The creek has low flow and when sampled, at the highest discharge, was no more than 15 cm deep and 30 cm wide. Two sites were sampled at the creek about five meters apart labeled 'upstream' and 'downstream' relative to the flow of the water. Over the course of the three days of sampling the water flow decreased substantially so that no water remained in the downstream sampling location on day 3.

Hand held sensors measured the pH (Cole Parmer), oxygen concentration and temperature (An IQ Scientific Instruments model IQ180GLP sensor); in this ecosystem, the voltammetry unit detected a significant Fe(III)-organic signal that overlapped and interfered with quantifying the oxygen signal. These waters contain significant humic material that stabilize soluble Fe(III). Voltammetric profiles were taken for redox species analysis without any other interference using the solid-state 100 μm Au glass working electrodes in conjunction with a DLK-60 electrochemical analyzer from Analytical Instruments Systems Inc. (AIS) (e.g., Ma et al 2006[26]). The microelectrode was mounted on a manually operated micromanipulator, which enabled high resolution profiling of up to 0.05 mm increments.

Plastic syringes with Teflon cannulas were used to sample water from just above the iron mat located about two cm below the surface and the water was immediately filtered through 0.2 μm pore-sized 25mm diameter filters, then acidified to pH = 2 to prevent any oxidation and returned to the laboratory for chemical analysis. Fe(II) and total dissolved Fe were determined using UV-Vis spectroscopy and the ferrozine method of Stookey (1970)[27]. Ferrous iron was determined in acidified samples by adding 3 mL of a 1:1 mixture of 0.01 M ferrozine and 6 M ammonium acetate buffer. After a waiting period of half an hour the absorbance at 562 nm was read. After the initial measurement of Fe(II) was made, the sample was conserved and 250 μL hydroxylamine was added to reduce Fe(III) to Fe(II) in order to measure total iron (e.g., Yücel et al, 2011)[28].

### 2.5 Cape Shores Sampling (July 7, 2013)

The Cape Shores beach is located at Cape Henlopen in Lewes, Delaware on the Delaware Bay (38˚47.13'N, 75˚6.27'W). Within the intertidal aquifer, fresh groundwater mixes with salt water. The iron content of freshwater is apparent at low tide, when iron-rich orange (Fe oxide) or black (FeS) freshwater seepage occurs on the beach surface. Heiss et al (2014),[29] previously installed eight multilevel wells in a transect perpendicular to shore. Sampling was done in July 2013, using a peristaltic pump to draw water from each well, each of which has multiple Teflon tubes of 0.25 inch diameter with the ends located at 3-5 depths ranging from 0.39 to 3.6 meters. Sampling began just after high tide with the wells closest to the upland part of the beach sampled first, and the seaward wells were sampled in succession as the ocean water receded. The sampling of all wells took about six hours. The water was pumped to a flow through electrochemical cell as described in Luther et al. (2002) and Konovalov et al (2003)[30] where the PEEK electrodes are used in conjunction with a field deployable DLK60 electrochemical analyzer to measure the redox chemistry. Once the water passed through the electrochemistry flow cell, it entered a second (100 mL) flow cell attached to a YSI Quatro cable with probes for pH, ORP (oxidation reduction potential), conductivity, temperature, and dissolved oxygen (DO) that provide data using a YSI Professional Plus hand held meter. Water samples from each well were also collected and filtered (Millipore Sterivex 0.22 µm pore size) for DNA extraction and analysis of small subunit ribosomal RNA (SSU rRNA) gene sequences. These filters were kept on ice until same day transfer to a laboratory freezer. The extraction velocity from each well was 3.4-5.8 mL/s for biogeochemical analysis and 13.2 mL/s for biological sampling.

### 2.6 Mid Atlantic Ridge Sampling (October 2012)

Three sites (Rainbow, TAG and Snakepit) on the Mid Atlantic Ridge (MAR) were sampled with the ROV Jason II during KN209-02 to the MAR in October- November 2012. Rainbow (36°13.80'N - 33°54.14'W) is situated at 2300 m depth. TAG (Trans-Atlantic Geotraverse; 26°08.2'N and 44°49.6'W, ~3700 m). and Snakepit (23 22.141342 N, 44 57.070219 and 23 22.120024 N, 44 57.126718 W) are both ~1000 m deeper than Rainbow. For this work, mats found near the vent sites were sampled and analyzed.

The PEEK electrodes were mounted in conjunction with a thermocouple inside a Delrin wand as described in Luther et al, (2001 and 2008[20]) and manipulated using the ROV Jason II. The wand also contained the titanium casing with the electronics of the DLK-III submersible electrochemical analyzer. The sensor communicated with a laptop on board ship via the Jason II fiber optic cable, and the scans were taken using software from the manufacturer (Analytical Instrument Systems, Inc).

Sets of ten cyclic voltammograms were collected by conditioning the electrode at the initial potential (-0.05 V) for 2 s, then scanning from -0.05 to -1.8 V and back to -0.05 V at a scan rate of 2 Vs-1. A conditioning potential at -0.9 V was applied for 5 s before the first scan of each set of ten scans as a way of ensuring a clean electrode surface. Temperature measurements were recorded simultaneously with each electrode scan. See Gartman et al (2011)[31] and Luther et al (2008)[20] for more details on *in situ* voltammetry at hydrothermal vents. Mat samples were obtained with an automatic syringe multi-sampler as described in Breier et al (2012)[32].

### 2.7. Culture methods for demonstrating microbial iron oxidation

FeOB were enriched in zero valent iron gradient plates or agarose-stabilized gradient tubes (using a bottom plug of $FeCO_3$ or $FeCl_2$) in artificial seawater (ASW) medium, modified Wolfe's mineral medium (MWMM), or a mixture of the two for estuarine samples, as per Emerson and Floyd (2005)[33]. Because $FeCO_3$ and $FeCl_2$ can only provide Fe(II) as an electron donor, the growth in the tubes must be based on Fe(II) oxidation. Growth was initially evaluated by looking for a sharp distinct orange growth band in gradient tubes or orange floc in gradient plates. Positive growth was confirmed by staining samples with SYTO13 (a fluorescent nucleic acid stain, Invitrogen) and observing cells by epifluorescence microscopy (Olympus BH2 or BX60 microscope).

### 2.8. Microbial community identity through SSU rRNA gene sequencing and qPCR

For Cape Shores samples, quantification of microbial community member abundance was accomplished through tagged pyrosequencing of the V1-V3 region of the SSU rRNA gene. DNA was extracted from samples using MoBio PowerSoil kits, and sent for amplification, tagging, and sequencing at the Research and Testing Laboratory (Lubbock, TX, USA) using a Roche 454 FLX system with Titanium chemistry (Roche, Nutley, NJ). Sequence quality filtering and classification were completed using the Qiime next generation sequencing pipeline (Caporaso et al., 2010[34]). Classified sequences were then screened for taxa known to oxidize iron.

Quantitative-PCR was also employed to specifically test for the marine iron-oxidizing Zetaproteobacteria. The details of primer design and experimental protocol for this method have been published elsewhere (Fleming et al., 2013[35]). Copy numbers of total bacteria (Bact 533F – Bact 684R) and Zetaproteobacteria (537F to 671R) SSU rRNA genes were quantified in 1 ng of genomic DNA using quantitation against a standard curve of linearized plasmids using Power SYBR Green reagents on a 7500 Fast Real-Time PCR System (Applied Biosystems, Foster City, CA, USA). Percentages of Zetaproteobacteria in the original genomic DNA were calculated by dividing the Zetaproteobacteria copy number by the total bacteria copy number.

## 3.0 Results and Discussions

### 3.1 Chesapeake Bay results

Using an *in situ* vertical profiler, figure 1 shows the profiles of the major redox parameters (oxygen and sulfide) and physical parameters (temperature and salinity) of the water column. In general, oxygen and temperature decrease with depth as salinity and sulfide increased with depth. Iron concentrations were below the detection limit of the electrochemical package; however, discrete

samples from the pump profiler system and the CTD system measured using the Ferrozine method indicate that Fe(II) concentrations ranged from 100 nanomolar to 3 micromolar. Both Fe(II) and (III) were detected in the suboxic zone, with a decrease in Fe(III) in the anoxic zone, and a corresponding increase in Fe(II). Figure 1a shows a suboxic zone in 2011 between 6 and 8 meters water depth where both oxygen and sulfide are not detectable (values plotted as '0' indicate the detection limit). Below 8 meters, $H_2S$ is present and Fe(II) increases. Ferrozine analyses of discrete samples indicate concentrations of Fe(II) up to 3.5 micromolar, which is less than the electrode detection limit of 7 μM. Because of the low oxygen concentrations and the presence of Fe(II), the depths that mark the transition from oxic to suboxic constitute an ideal zone to search for FeOB. Samples from this region were used as inoculum for enrichment of FeOB using agarose-stabilized gradient tubes with either $FeCl_2$ (Figure 1b) or $FeCO_3$ substrates. Positive cultures for FeOB were found at multiple depths during the Chesapeake cruises in both 2011 and 2013. In Figure 1(A) the star located at a depth of 6.3 meters indicates one of the positive cultures for FeOB (star in Figure1B). Figure 1(C) shows a voltammetric profile from the Chesapeake cruise in 2013, with positive cultures for FeOB found at multiple depths (12, 13.4, 13.8, and 14 meters). Fe(III) oxide-depositing organisms grew in these cultures, demonstrating the presence of FeOB. Also shown in Figure 1(B) is a control sample from the fully oxygenated surface waters of the Chesapeake Bay, where no FeOB were found. Figure 1c shows a similar suboxic zone in 2013 as was found in 2011 using the pump profiling system; because FeOB were found during both time periods, they are likely a common feature in this ecosystem.

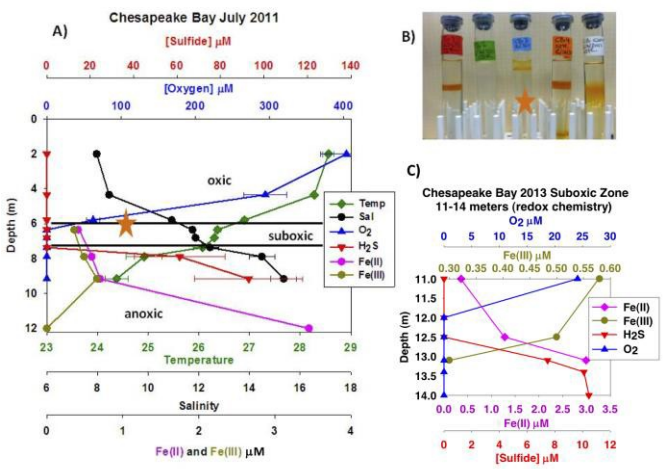


**Figure 1.** (a) Representative vertical profile from the Chesapeake Bay in July of 2011 with sulfide, oxygen, Fe(II), Fe(III), temperature, and salinity plotted vs depth with each chemical zone (oxic, suboxic, and anoxic) shown;(b) Images of $FeCl_2$ gradient tube cultures. Three tubes show distinct, sharp orange bands, indicating positive FeOB growth from the Chesapeake Bay. The right-most tube is the uninoculated control, showing a diffuse orange band, indicating abiotic Fe(II) oxidation; (c) Fe(II), Fe(III), $O_2$, and $H_2S$ concentrations found around the suboxic zone from the Chesapeake cruise in 2013.

**Catalytic cycle**

A question arises from these data, how do these iron-oxidizing bacteria survive in a low oxygen and low iron concentration zone like this suboxic zone? The physics of this zone allows for a low but constant supply of reduced iron and sulfide to its bottom, while at the same time there is a continuous and low supply of oxygen approaching from the top. At this point, there are three chemical reactants that can be measured and react with each other to set up a catalytic cycle. Abiotic Fe(II) oxidation is very slow at low oxygen concentrations allowing for iron-oxidizing bacteria to mediate Fe(II) oxidation under low oxygen conditions as previously shown by Druschel et al (2008)[9] and Rentz et al (2007)[8]. Although we do not have rates for biotic Fe(II) oxidation, we have identified positive cultures of FeOB indicating that they are present immediately above and below as well as in this suboxic zone. Once Fe(II) oxidizes, it becomes iron (III) oxyhydroxide solids that will fall in the water column to the sulfidic zone. Here the solids will be re-reduced to soluble Fe(II) and perhaps nanoparticulate FeS, which in turn diffuse back up to the suboxic zone and then be re-oxidized by oxygen mediated by the iron oxidizing bacteria. Our electrochemical method allows for the determination or detection of both Fe(II) and nanoparticulate FeS. Because sulfide is prevalent in the bottom waters of the Chesapeake Bay at different times of the year, Fe(II) reacts with sulfide to form iron sulfide particulate and nanoparticulate phases so aqueous Fe(II) does not build up into very high concentrations as in other sites reported elsewhere in this paper. Our electrochemical method indicated that nanoparticulate FeS was present in many samples, but could not be quantified as there is no standard for nanoparticulate FeS[20].

Thus, the Chesapeake Bay is a unique site in the context of this study because the suboxic zone allows for a biogeochemical catalytic cycle to occur as has been shown in other sites[26]. An important feature of this catalytic cycle is that it allows for particularly low concentrations of Fe(II), oxygen and sulfide; these conditions can be ideal if the turnover of the catalytic cycle is high so that organisms can reuse Fe(II) as if they were experiencing a high concentration of Fe(II). Existing laboratory kinetic studies on Fe(II) oxidation with oxygen demonstrated that abiotic oxidation became much less important at low oxygen concentrations. To date laboratory kinetic studies have only been performed with 10 micromolar oxygen as the lowest concentration[9]. In the suboxic zone, Fe(II) oxidation is occurring even at concentrations less than the detection limit of our voltammetry system of 3 μM $O_2$ and 7 μM for Fe(II). Gradient tube methods that are commonly used[36,37] show a similar decrease in oxygen and a decrease in iron at the interface, creating an opposing gradient where both Fe(II) and $O_2$ can be found at very low concentrations (with high FeOB numbers), similar to what we observe here in a natural habitat, the Chesapeake Bay.

**Mid Atlantic Ridge Vent Sites**

Using the high definition cameras aboard the ROV Jason, we were able to locate yellow-orange microbial mats at three different hydrothermal vent sites at the Mid Atlantic Ridge (Rainbow, TAG, and Snakepit). These were discretely sampled using a syringe sampler specifically designed for deep-sea microbial mat sampling (Breier, et al 2012[32]). Microscopic analysis of these mats confirmed that morphotypes (Fe-encrusted stalks and sheaths) indicative of marine FeOB were common and abundant in all the mats collected at the different MAR sites (Emerson & Moyer, 2010). A high throughput phylogenetic analysis showed they all had a high relative abundance of Zetaproteobacteria (J. Scott, et al. manuscript in preparation). Voltammetric data were collected immediately before and after mat sampling to characterize the environment in which the mat was found. Table 1 shows $O_2$ and $Fe^{2+}$ data from each of the three vent sites. At each vent site, dissolved oxygen concentrations immediately above the mat ranged between 78-152 μM($O_2$ saturations were 45% or less at these temperatures), whereas $Fe^{2+}$ averaged about 25 μM for Snakepit and TAG. Quantitative Fe(II) measurements at Rainbow mat sites were not achievable as the reference electrode became compromised due to an electrode boot failure that allowed seawater to penetrate the connection thus causing a negative potential shift in the signals over time; however of the three sites sampled, Rainbow has the highest concentrations of iron in end-member vent fluid[38]. All chemical species were detected above the surface of the mat and there was an increase in temperature above the mat suggesting fluid flow from the sediment through the mat. These data suggest there is a net positive flux of Fe(II) through the mat, and that the FeOB capitalize on these $O_2$ poor and Fe(II)-rich waters for growth. How much Fe(II) they remove from the overall flux through the mats remains an unknown.

**Table 1**. Fe(II) and $O_2$ data from the three different vent sites.

| Vent Site | [$O_2$] μM | [$Fe^{2+}$] μM |
|---|---|---|
| Rainbow | 108.25 | N/A |
| Snakepit | 78.08 | 26.33 |
| TAG | 151.25 | 23.34 |

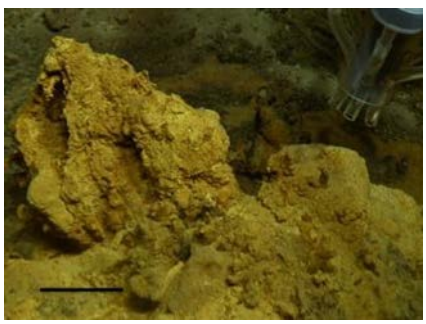

**Figure 2**. Image of microbial mat (with the tip of the syringe sampler) near the Rainbow vent site. Marker bar = 5cm

**Cape Shores**

At Cape Shores Beach, groundwater flow provides a flux of Fe(II) into a subsurface intertidal mixing zone, where freshwater mixes with saline ocean water. The salinity, Fe(II) and $O_2$ gradients created in this mixing zone should provide a favorable environment for both marine and freshwater FeOB. All contour plots in Figure 3 (A) show a blue line above each chemical parameter that represents the slope of the beach. The high salinity at the left most well is due to a channel (marked by a diamond) that allows seawater at high tide to build up and then infiltrate the beach sands. Groundwater flow is generally from left to right, with vertical flow and discharge to the surface around Well 12 (see details in Heiss et al., 2014[19]). The contour plots in Figure 3(A) shows changes in salinity, $O_2$, Fe(II), and Fe(III), emphasizing hot spots of Fe and $O_2$ , and salinity gradients. These two-dimensional contour plots help to identify areas in which redox conditions would favor FeOB. Salinity, which is a conservative tracer of seawater, shows the mixing patterns of fresh and saline water. The zones of highest salinity had the highest $O_2$ concentrations (up to 70 μM) whereas the fresh groundwater had $O_2$ below the 6.25 μM detection limit of the YSI handheld $O_2$ meter; this indicates that infiltrating ocean water is the primary source of $O_2$. The $O_2$ handheld meter was used where there were interferences and where the $O_2$ peak could not be measured. Both Fe(II) and Fe(III) were present in the groundwater and as it mixed with partially oxygenated seawater, Fe(II) almost completely oxidized to Fe(III) including a soluble form of Fe(III) that overlapped the $O_2$ voltammetric peak. Also shown in Figure 3(A) are sulfide concentrations for each well. Sulfide measurements are important as Fe(II) reacts readily with sulfide to form particulate and nanoparticulate iron(II) sulfides, thus keeping free Fe(II) concentrations low. Figure 3(B) shows a plot of Fe(II), Fe(III), $O_2$, and % Zetaproteobacteria (by qPCR) versus depth (m) for well 12; here we see that FeOB (represented by Zetaproteobacteria) are at an Fe(II)/Fe(III) interface where $O_2$ is less than 10 μM. Additionally, by high throughput pyrosequencing of all July 2014 porewater samples, iron oxidizers were detected at low levels in several porewater samples throughout the site and constituted up to 3% of the bacterial community for sampling done across all eight wells.

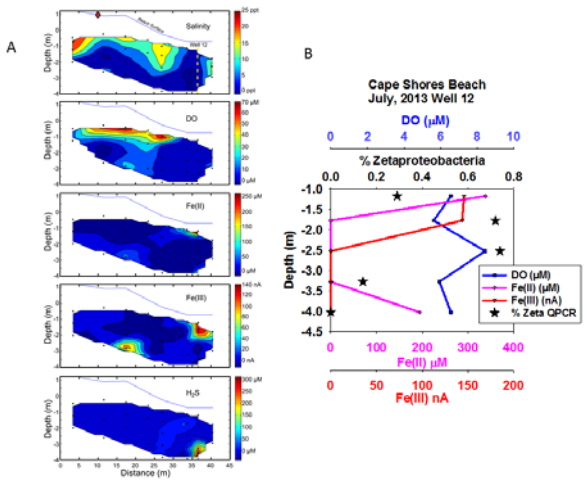


**Figure 3**. (a) Contour plots showing changes in salinity, dissolved oxygen (DO), Fe(II), Fe(III), and $H_2S$ with depth as well as distance from the benchmark in the dunes. Black dots represent well sampling depths, while the blue line indicates the beach surface,

sloping towards the ocean. Well 12, shown in (b), is indicated with a dashed yellow line. (b) Well 12 profiles of DO, Fe(II), Fe(III) plots from Cape Shores July 2013 with % Zetaproteobacteria versus well depth (depth below beach surface).

Salinity and $O_2$ measurements are of particular importance here as the saline ocean water is oxygenated, and when mixed with the freshwater discharge, the source of Fe(II) can create favorable opposing gradients of both $O_2$ and Fe(II). The beach intertidal site is easily accessible but understudied as a habitat for FeOB. It differs from the other field sites in that water flow directions, and therefore chemical inputs and reaction zones, are spatially complex across the mixing zone. Since gradient directions cannot be inferred easily, tracking vertical and horizontal changes in redox-active solute concentrations at this beach site provides invaluable information on the locations of conditions that would support FeOB. Specifically FeOB were found in this ecosystem in areas with < 70 μM $O_2$ and frequently < 10 μM $O_2$.

**Lakeside drive (7/17/12-7/19/12)**

Lakeside Drive is a small freshwater stream that often contains high concentrations of Fe(II) that leads to abundant formation of microbial iron mats. The stream is surrounded by soils that are dense with decomposing organic matter and are anoxic, see ref 7 for more details about this site. These organic rich waters retain Fe(II) and Fe(III) in solution despite circumneutral pH and oxygenation[25]. Figure 4 shows two vertical profiles at the different sampling sites. These profiles are taken through the standing water where the mats were located. The upstream site (Profile 2) was taken in a small pool about 30 cm deep, where a mix of subterranean and surface water flowing through a marshy area forms the stream proper. The downstream site (Profile 1) was taken about 5 m further downstream where the water had more mixing time to become oxygenated. Profile 2 in Figure 4 shows a peak in both Fe(II) and Fe(III) at approximately 10 millimeters, and Fe(II) concentrations exceeded 200 μM at 70 mm below the surface. Oxygen concentrations at the upstream site averaged 68 μM $O_2$. Profile 1 from the downstream site shows no detectable iron [both Fe(II) and Fe(III)] below 2 mm with average $O_2$ concentrations of 85 μM. This loss of Fe(II) and Fe total shows the effects of mixing or reaction time of $O_2$ reacting with Fe(II) as the water is flowing.

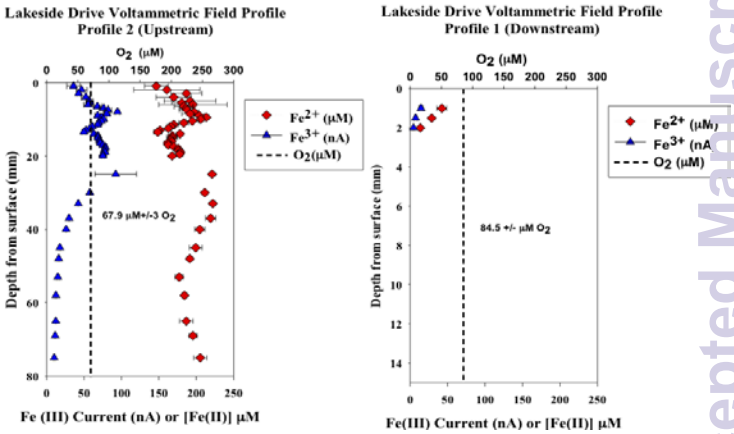


**Figure 4**. Profiles of Fe(II), Fe(III) and $O_2$ from the upstream and downstream sampling sites from Lakeside Drive, ME.

Table 2 shows Fe(II) and Fe total data from discrete samples, as opposed to voltammetric measurements shown above. At the upstream site the Fe(II) on 7/17/12 was 181 μM, in agreement with the voltammetric data, and the $O_2$ was 67.9 μM. The Fe(III) concentration at the upstream site was 7.51 μM. This value is almost 100x more than the estimate of what would be the instantaneous abiotic Fe(III) production or Fe(II) loss by abiotic oxidation of 88.2 nM calculated using the kinetics expression given in equation 1 with the values given in Table 2. The rate of Fe(II) loss shown in Table 2 comes from a single calculation with the values of [$Fe^{2+}$], [$O_2$], and pH listed. Thus, these calculations and the presence of FeOB indicates biological mediation of Fe(II) oxidation is more important than chemical oxidation.

**Table 2**. Lakeside Drive data and abiotic rate calculations for Fe(II) oxidation using equation 1.

| | Upstream 7/17/12 | Downstream 7/17/12 |
|---|---|---|
| [$Fe^{2+}$] | 181 μM | 145 μM |
| [$O_2$] | 67.9 μM | 84.5 μM |
| pH | 6.19 | 6.39 |
| Rate of [$Fe^{2+}$] Loss ($min^{-1}$ $mol^{1}$ $liter^{-1}$) | -8.82E-08 | -2.22E-07 |

Previous SSU rRNA gene sequence data show the presence of FeOB *Gallionellaceae* and *Leptothrix* at Lakeside Drive[39]. When the voltammetric profiling was done, the dominant morphotype in the iron mats was the sheath-forming *Leptothrix ochracea*. *L. ochracea* has been shown to be tolerant of higher $O_2$ concentrations than other FeOB[40], and requires Fe(II) for growth. It also produces copious amounts of Fe-oxide encrusted sheaths, most of which are empty, but form the matrix of the mat with a very high surface area. Thus it is not surprising that steady oxygen concentrations of 68 ± 10 μM were present where Leptothrix *ochracea* was actively growing [40]. The combination of high $O_2$ and Fe(II) concentrations along with a large surface area of Fe-oxide that can react with dissolved organic material to form dissolved Fe(III) complexes could well explain the increase of Fe(III) in the surrounding waters.

## Conclusions

This work shows that *in situ* voltammetry can be used to identify two broad chemical conditions where FeOB can be found; (1) sites where lower $O_2$, Fe(II) and $H_2S$ concentrations overlap to setup a catalytic cycle to sustain Fe(II)/Fe(III) interconversion, and (2) sites that have opposing vertical and/or horizontal $O_2$ and Fe(II) gradients.

Measuring redox species simultaneously with one electrode rather than a suite of sensors provides large advantages when searching for FeOB. Areas of favorable conditions can be located with greater resolution (due to small electrode size) and more accurate assessments of the redox chemistry in real time can be made (as opposed to laboratory/shipboard analysis where sample collection is required). Here we show FeOB in a variety of freshwater and marine environments with low $O_2$ ranging from below the 3 μM detection limit of the electrodes at the Chesapeake Bay suboxic zone [with Fe(II) up to 3 μM] to 150 μM $O_2$ at the MAR vent site [with Fe(II) up to 25 μM]. At the Cape Shores beach, $O_2$ was < 70 μM, and frequently <10 μM where as Fe(II) reached as high as 300 μM. Lastly, Lakeside drive showed $O_2$ up to 85 μM and Fe(II) as high as 250 μM. Evidence of FeOB at each site was described, and based on the *in situ* voltammetry and the biological data from discrete sample collection, we showed that biotic Fe(II) oxidation does occur in these environments. Thus, FeOB could play an important role in Fe(II) oxidation in diverse modern environments from terrestrial to coastal to deep sea. Further, with the ability to thrive at very low to moderate $O_2$ concentrations at circumneutral pH, FeOB were likely active contributors to Fe(III)-oxide formation in such habitats during the initial oxidation of the ancient oceans. In this work, we have shown many diverse environments where FeOB are found; the suboxic zone of the Chesapeake Bay may more closely match the type of oxygen environment hypothesized in the ancient oceans before the great oxidation event.

## Acknowledgements

This research was supported by the following grants: NASA: NNX12AG20G (to CSC, GWL and DE), NSF CAREER: EAR- 1151682 and NSF Bio Oce: OCE- 1155290 (to CSC); NSF Marine Geology and Geophysics: OCE-1131109 (to GWL); and NSF IOS-0951077 and NSF OCE-1155754 (to DE). We thank Holly Michael and James Heiss for Cape shores well access, field assistance, and discussion.

# References

1. Unnars, A., Lomqvist, S., Ohansson, P.. & Ndersson, C. *Geochimica et Cosmochimica Acta*, 2002, **66,** 745–758.
2. Deng, Y., Stumm, W. *Applied Geochemistry*, 1994, **9**, 23-36.
3. Kappler, A., Pasquero, C., Konhauser, K. O. & Newman, D. K.. *Geology, 2005*, **33,** 865.
4. Koehler, I., Konhauser, K. & Kappler, A. *Geomicrobiology: Molecular and Environmental Perspective*, 2010, 309–324.
5. Edwards, K. J. *et al. ISME J.*, 2011, **5,** 1748–58.
6. Emerson, D. & Moyer, C. L. Applied and Environmental Microbiology. 2002, **68,** 3085–3093.
7. F. Widdel et al., *Letters to Nature*, 1993, **362**, 834.
8. Rentz, J. A, Kraiya, C., Luther, G. W. & Emerson, D., *Environ. Sci. Technol.*, 2007, **41,** 6084–9.
9. Druschel, G. K., Emerson, D., Sutka, R., Suchecki, P. & Luther, G. W., *Geochim. Cosmochim. Acta*, 2008, **72,** 3358–3370.
10. Krepski, S. T., Hanson, T. E. & Chan, C. S., *Environ. Microbiol.*, 2012, **14,** 1671–80.
11. Yu, R., Gan, P., Mackay, A. A, Zhang, S. & Smets, B. F., *FEMS Microbiol. Ecol*., 2010, **71,** 260–71.
12. Roden, E. E. *et al.*, *Front. Microbiol.*, 2012, **3,** 172.
13. Lüdecke, C., Reiche, M., Eusterhues, K., Nietzsche, S. & Küsel, K. *Environ. Microbiol.*, 2010, **12,** 2814–25.
14. Emerson, D., Fleming, E. J. & McBeth, J. M., *Annu. Rev. Microbiol.*, 2010, **64,** 561–83.
15. Krepski, S. T., Emerson, D., Hredzak-Showalter, P. L., Luther, G. W. & Chan, C. S., *Geobiology*, 2013, **11,** 457–71.
16. Chan, C. S., Fakra, S. C., Emerson, D., Fleming, E. J. & Edwards, K. J. *ISME J.* , 2011, **5,** 717–27.
17. Hedrich, S., Schlömann, M. & Johnson, D. B. , *Microbiology*, 2011, **157,** 1551–64 .
18. Trouwborst, R. E., Johnston, A., Koch, G., Luther, G. W. & Pierson, B. K., *Geochim. Cosmochim. Acta*, 2007, **71,** 4629–4643.
19. Mullaugh, K. M. *et al.*, *Electroanalysis*, 2008, **20,** 280–290.

20. Luther, G. W. *et al.* , *Mar. Chem.*, 2008, **108,** 221–235.

21. Weiss, R., *Deep Sea Research and Oceanographic Abstracts*, 1970, **17,** 721–735.

22. Taillefert, M., Bono, a. B. & Luther, G. W., *Environ. Sci. Technol.*, 2000, **34,** 2169–2177.

23. Brendel, P. J. & Luther, G. W. , *Environ. Sci. Technol.*, 1995, **29,** 751–61.

24. Suggett, D., Moore, C., Hickman, A. & Geider, R., *Marine Ecology Progress Series*, 2009, **376,** 1–19.

25. Fleming, E. J., Cetinić, I., Chan, C. S., Whitney King, D. & Emerson, D., *ISME J.* , 2013, 1–12

26. Ma, S., Noble, A., Butcher, D., Trouwborst, R. E. & Luther, G. W., *Estuar. Coast. Shelf Sci.*, 2006, **70,** 461–472.

27. Stookey, L. L., *Anal. Chem.*, 1970, **42,** 779–781.

28. Yücel, M., Gartman, A., Chan, C. S. & Luther, G. W. , *Nat. Geosci.*, 2011, **4,** 367–371.

29. Heiss, J.W., Ullman, W.J, Michael, H.A. *Estuarine, Coastal and Shelf Science*, 2014.

30. Konovalov, S. K. *et al.*, *Limnol. Oceanogr.*, 2003, **48,** 2369–2376.

31. Gartman, A. *et al.*, *Aquat. Geochemistry*, 2011, **17,** 583–601.

32. Breier, J. A., Gomez-Ibanez, D., Reddington, E., Huber, J. A. & Emerson, D., *Deep Sea Res. Part I Oceanogr. Res. Pap.*, 2012, **70,** 83–90.

33. Emerson, D. & Floyd, M. M., *Methods Enzymol.*, 2005, **397,** 112–23.

34. Caporaso, J. G. *et al.*, *Nat. Publ. Gr.*, 2010, **7,** 335–336.

35. Fleming, E. J. *et al.* , *FEMS Microbiol. Ecol.*, 2013, **85,** 116–127.

36. Roden, E. E., Sobolev, D., Glazer, B. & Luther, G. W., *Geomicrobiol. J.*, 2004, **21,** 379–391.

37. Emerson, D., Weiss, J. V & Megonigal, J. P., *Applied and Environmental Microbiology*, 1999, **65,** 2758-2761.

38. Laney, S. R. Chlorophyll a Fluorescence in Aquatic Sciences: Methods and Applications. 19–31 (2010). doi:10.1007/978-90-481-9268-7

39. Fleming, E. J. *et al.*, *PLoS One*, 2011, **6,** e17769.

40. Emerson, D. & Revsbech, N. P., *Appl. Environ. Microbiol.*, 1994, **60,** 4022–31.